

Terrestrial responses of low-latitude Asia to the Eocene–Oligocene climate transition

Y.-X. Li et al.

Terrestrial responses of low-latitude Asia to the Eocene–Oligocene climate transition revealed by integrated chronostratigraphy

Y.-X. Li¹, W. Jiao¹, Z. Liu², J. Jin³, D. Wang⁴, Y. He⁵, and C. Quan⁶

¹State Key Laboratory for Mineral Deposits Research, School of Earth Sciences and Engineering, Institute of Geophysics and Geodynamics, Nanjing University, Nanjing 210046, China

²Department of Earth Sciences, The University of Hong Kong, Hong Kong, China

³State Key Laboratory of Biocontrol and Guangdong Key Laboratory of Plant Resources, School of Life Sciences, Sun Yat-sen University, Guangzhou 510275, China

⁴College of Earth Sciences, Jilin University, Changchun 130061, China

⁵Department of Earth Sciences, Zhejiang University, Hangzhou, China

⁶Research Center of Paleontology and Stratigraphy, Jilin University, Changchun 130026, China

Title Page

Abstract

Introduction

Conclusions

References

Tables

Figures

◀

▶

◀

▶

Back

Close

Full Screen / Esc

Printer-friendly Version

Interactive Discussion

Received: 01 May 2015 – Accepted: 15 June 2015 – Published: 08 July 2015

Correspondence to: Y.-X. Li (yxli@nju.edu.cn), C.Quan (quan@jlu.edu.cn)

Published by Copernicus Publications on behalf of the European Geosciences Union.

CPD

11, 2811–2845, 2015

**Terrestrial responses
of low-latitude Asia to
the
Eocene–Oligocene
climate transition**

Y.-X. Li et al.

Title Page

Abstract

Introduction

Conclusions

References

Tables

Figures



Back

Close

Full Screen / Esc

Printer-friendly Version

Interactive Discussion



Abstract

The Paleogene sedimentary records from southern China hold important clues to the impacts of the Cenozoic climate changes on low-latitudes. However, although there are extensive Paleogene terrestrial archives and some contain abundant fossils in this region, few are accurately dated and have a temporal resolution adequate to decipher climate changes. Here we present a detailed stratigraphic and paleomagnetic study of a fossiliferous late Paleogene succession in the Maoming Basin, Guangdong Province. The succession consists of oil shale of the Youganwo Formation (Fm) in the lower part and massive pebbly coarse sandstones of the overlying Huangniuling Fm in the upper part. The conformable transition from oil shale to sandstones represents a major depositional environmental change from a lacustrine to a deltaic environment. The substantially refined chronostratigraphic framework is established based on the litho-, bio-, cyclo-, and magnetostratigraphic data that place the environmental transition at 33.88 Ma, coinciding with the Eocene–Oligocene climate transition (EOT) at ~ 33.7 to ~ 33.9 Ma. We suggest that the transition from a lacustrine to deltaic environment in Maoming Basin represents terrestrial responses to the EOT and indicates a significant reduction in hydrodynamics in low-latitude regions during the global cooling at EOT.

1 Introduction

The Late Paleogene witnessed one of the most prominent climatic changes in the Cenozoic, a transition from greenhouse to icehouse world. The transition is climaxed at the Eocene–Oligocene boundary when marine sediments registered a large, widespread, and rapid cooling in oceans (e.g., Zachos et al., 2001; Liu et al., 2009; Bohaty et al., 2012), which was accompanied by a sudden deepening of the carbonate compensation depth (CCD) by ~ 1.2 km (Pälike et al., 2012) in oceans and a severe calamity in the marine community that gave rise to the largest marine mass extinction since the end of Cretaceous (e.g., Prothero, 1994; Pearson et al., 2008; Cotton and

CPD

11, 2811–2845, 2015

Terrestrial responses of low-latitude Asia to the Eocene–Oligocene climate transition

Y.-X. Li et al.

Title Page

Abstract

Introduction

Conclusions

References

Tables

Figures

◀

▶

◀

▶

Back

Close

Full Screen / Esc

Printer-friendly Version

Interactive Discussion

Terrestrial responses of low-latitude Asia to the Eocene–Oligocene climate transition

Y.-X. Li et al.

Title Page

Abstract

Introduction

Conclusions

References

Tables

Figures



Back

Close

Full Screen / Esc

Printer-friendly Version

Interactive Discussion

Pearson, 2011). On land, this transition is expressed as rapid ice sheet growth over Antarctic (e.g., DeConto and Pollard, 2003; Coxall et al., 2005; Goldner et al., 2014) and large-scale cooling (e.g., Zanazzi et al., 2007; Dupont-Nivet et al., 2007; Hren et al., 2013). While the transition is widely recognized in the marine realm (Zachos et al., 2001; Jovane et al., 2006; Liu et al., 2009; Pälike et al., 2012; Westerhold et al., 2014) and is increasingly well-defined in terrestrial records from the Atlantic region (e.g., Zanazzi et al., 2007; Hren et al., 2013), its impacts on Asian environment remain poorly understood. This is largely because the concomitant tectonism, i.e., the Tibetan plateau uplift, and the development of monsoonal climate may also impose strong influence on Asian environment (e.g., Dupont-Nivet et al., 2007; Quan et al., 2012, 2014; Wang et al., 2013; Licht et al., 2014, 2015; Shukla et al., 2014).

There are numerous basins in southern China that host conspicuous Cenozoic sedimentary archives documenting the Cenozoic climate changes in the region. The late Paleogene sedimentary records from this region are of particular interest because they hold clues to the dramatic shift of climates in low-latitude Asia (Quan et al., 2012; Wang et al., 2013; Licht et al., 2014, 2015), where the influence of the Tibetan Plateau uplift should be minimal in comparison to the Asian interior. However, although abundant Paleogene sedimentary successions were developed here (e.g., Tong et al., 2005, 2013), their age controls are generally poor. Despite the fact that some successions contain vertebrate and/or plant fossils (e.g., Tong et al., 2005, 2013), the indicative age ranges of these fossils are often too broad to date climate changes with satisfactory accuracy and precision.

In this paper, we present a detailed stratigraphic and paleomagnetic study on the fossiliferous Eocene to Oligocene succession in the Maoming Basin of Guangdong Province, southern China to construct a new chronostratigraphic framework that is based on an integrated litho-, bio-, magneto-, and cyclostratigraphy. The new chronology not only greatly reduces the uncertainty but also significantly refines the available fossil-based timescale of the succession. In particular, the substantially refined chronology permits establishing the link between the dramatic environmental change in the

to Oligocene, or even to the Miocene (Yu and Zu, 1983; Wang et al., 1994; Guo, 2006; Aleksandrova et al., 2012).

Facies analysis indicates that the Youganwo Fm was formed in a lacustrine environment, while the overlying Huangniuling Fm was deposited in a deltaic environment (Guo, 2006). The transition from a lacustrine environment to a deltaic environment indicates reduced hydrodynamic conditions that may be associated with regional climate changes as inferred from other parts of southern China (Wang et al., 2013). However, because the ages of the two formations are poorly constrained, age estimates for the Youganwo–Huangniuling boundary can be as large as over 10 Myrs, ranging from the Late Eocene to the Miocene, which makes it difficult to relate the transition to any major climate events. Although a paleomagnetic work of drill cores from the Maoming Basin (Wang et al., 1994) constructed a magnetic polarity timescale, the study was mainly focused on the Huangniuling Fm and younger units. Also, the mean sampling spacing is large, ~ 2.6 m, and changes in sedimentation rates as indirectly reflected by the lithology were not taken into account. The magnetic polarity timescale can only be regarded as preliminary by modern standards.

3 Methods

The study section is well exposed in the cliffs of the now-abandoned open mine pit (21°42.3' N, 110°53.9' E), located to the northwest of the Maoming City (Fig. 1). The exposed section comprises the upper part of the Youganwo Fm and the overlying Huangniuling Fm. To detect subtle changes in lithology of the exposed Youganwo Fm, magnetic susceptibility was measured with a hand-held susceptibility meter SM30, typically at every 10 to 20 cm. For the overlying Huangniuling Fm, its basal 30 m was measured and major lithological changes in its upper part are noted.

Oriented paleomagnetic samples were collected from the exposed Youganwo Fm and the lower part of the overlying Huangniuling Fm at the center of the basin where the gradual transition between the two formations occurs (see Sect. 4.1). For oil shales

Terrestrial responses of low-latitude Asia to the Eocene–Oligocene climate transition

Y.-X. Li et al.

Title Page

Abstract

Introduction

Conclusions

References

Tables

Figures

◀

▶

◀

▶

Back

Close

Full Screen / Esc

Printer-friendly Version

Interactive Discussion



**Terrestrial responses
of low-latitude Asia to
the
Eocene–Oligocene
climate transition**

Y.-X. Li et al.

[Title Page](#)[Abstract](#)[Introduction](#)[Conclusions](#)[References](#)[Tables](#)[Figures](#)[◀](#)[▶](#)[◀](#)[▶](#)[Back](#)[Close](#)[Full Screen / Esc](#)[Printer-friendly Version](#)[Interactive Discussion](#)

in the Youganwo Fm, samples were collected usually every ~ 30 to 40 cm and, where possible, 2 core samples were taken from a stratigraphic level. For the Huangniuling Fm, samples were mainly collected from the interbedded thin, gray mudstones. A gasoline-powered portable rock drill was used to collect samples and a Pomery orientation device was used to orient the samples. Oriented block samples were taken from outcrops where drilling is not possible. A total of 109 core samples and 66 block samples from 122 stratigraphic levels were collected from this section.

In the laboratory, the samples were trimmed to standard cylindrical paleomagnetic specimens or cut into 2 cm × 2 cm × 2 cm cubes. Anisotropy of magnetic susceptibility (AMS) of all specimens was measured with a KLY-3 Kappabridge. The specimens were then subjected to progressive thermal or AF (alternating field) demagnetization. The AF demagnetization was performed with a Molspin demagnetizer and the thermal demagnetization was conducted with an ASC TD48 thermal demagnetizer. The remanence of specimens was measured with a three-axis, 2G Enterprise Inc. 755 rock magnetometer. To constrain the magnetic mineralogy, isothermal remanent magnetization (IRM) acquisition was conducted with an ASC impulse magnetizer (IM-30) for selected samples. In the IRM acquisition experiments, each sample was magnetized in a forward field that progressively increases from 20 mT to 1.2 T. The sample was then progressively demagnetized in a backward field to estimate the coercivity of magnetic minerals. Between each magnetization/demagnetization treatment, the remanence of the sample was measured with an AGICO JR6A magnetometer. To further aid in magnetic mineralogy determination, thermal changes of magnetic susceptibility of two samples from the Youganwo Fm were measured with a MFK Kappabridge at the Paleomagnetism Laboratory of Chinese Academia of Science. The magnetic susceptibility of the samples was measured while the samples were heated and cooled between the room temperature and 700 °C in an argon environment. All the demagnetization experiments and remanence measurements were conducted in a magnetically shielded room (residual field < 300 nT) in the Paleomagnetism Laboratory of Nanjing University, China.

The demagnetization data were analyzed using the principal component analysis technique (Kirschvink, 1980). The demagnetization data are presented graphically with vector end point diagrams (Zijderveld, 1967). Software packages Puffinplot (Lurcock and Wilson, 2012) and PMGSC (by Randy Enkin) were used for paleomagnetic data analysis. The defined polarity zones, together with constraints from the paleontologic and lithologic data, are compared with the Geomagnetic Polarity Time Scale (GPTS) of Ogg (2012) to establish a chronologic framework for the investigated section.

4 Results

4.1 Sedimentary rhythms

The lithostratigraphy of the investigated section is summarized in Fig. 2. The lithology difference of the Youganwo Fm at the lower part and the Huangniuling Fm at the upper part of the section is dictated by the distinct color contrast (Fig. 2c–e). The overall light brownish color in the lower part characterizes the exposed Youganwo oil shale, while the overall pale grey to light yellowish color in the upper part characterizes the overlying, sandstone-dominated Huangniuling Fm (Fig. 2e). One of the most striking features of the outcrop is the occurrence of sedimentary rhythms, which are impressively expressed as the repeated occurrence of beds with distinct reddish color, in both the Youganwo Fm and the Huangniuling Fm (Fig. 2c and e). In the Youganwo Fm, there are more than a dozen of beds displaying distinct reddish color (Fig. 2a). The sedimentary rhythm is particularly well expressed between ~ 11 and 30 m, where the average spacing between two neighboring reddish beds is about 1.0 to 1.5 m (Fig. 2a). Magnetic susceptibility (MS) data can facilitate the characterization of sedimentary rhythms in the Youganwo Fm. High-resolution MS measurements show that the MS peaks generally correspond to the beds with reddish color and also exhibit meter-scale cyclicity (Fig. 2b). Close inspection of the beds with reddish color found that the reddish coloration represents weathering banding of the beds because fresh exposure of

Terrestrial responses of low-latitude Asia to the Eocene–Oligocene climate transition

Y.-X. Li et al.

Title Page

Abstract

Introduction

Conclusions

References

Tables

Figures

◀

▶

◀

▶

Back

Close

Full Screen / Esc

Printer-friendly Version

Interactive Discussion



these beds does not show reddish color. Regardless of the origin of the reddish color, its meter-scale rhythmic occurrence exemplifies subtle compositional changes of the Youganwo oil shale in a repeated fashion, which could be due to cyclic variations in the depositional environment during oil shale formation in the Maoming Basin.

5 In the Huangniuling Fm, the distinct red layer consists of coarse sandstones. It occurs at the base of the pale grey massive coarse sandstone and is typically a few centimeters thick. Because it is much more consolidated than the rest of the massive sandstones, the basal red sandstones are more resistant to weathering than the rest of the massive sandstones and commonly stick out of the surface of the outcrop, making the distinct red layers readily recognizable at distance (Fig. 2c). The thickness of the massive sandstone varies largely from decimeters to meters, occasionally up to decameters. Above massive sandstones is typically a relatively thinner mudstone bed (Fig. 2c). A red layer, massive sandstones, and a thin mudstone bed appear to form a parasequence that occurs repeatedly across the Huangniuling Fm (Fig. 2a–c). Using the distinct red layer as a marker bed, we have counted 19 parasequences, representing 19 sedimentary cycles, in the exposed Huangniuling Fm (Fig. 2a and b).

The contact between the Youganwo Fm and the overlying Huangniuling Fm is sharp at many locations around the edge of the open mine pit where coarse sandstones of the Huangniuling Fm directly sit atop of brown grey to dark grey mudstones of the upper part of the Youganwo Fm. However, when the contact is traced to the center of the basin, the transition is represented by a ~ 50 cm thick layer that displays a continuous, gradual change from brown grey mudstones at the uppermost Youganwo Fm to pale grey mudstones at the base of the Huangniuling Fm (Fig. 2d). Above the pale grey mudstone are siltstones and sandstones, exhibiting a coarsening upward trend in grain size. These features suggest that the deposition was continuous at the study site when the Maoming Basin experienced the transition from a lacustrine environment as represented by the Youganwo Fm to a deltaic environment as represented by the Huangniuling Fm (Guo, 2006).

Terrestrial responses of low-latitude Asia to the Eocene–Oligocene climate transition

Y.-X. Li et al.

[Title Page](#)[Abstract](#)[Introduction](#)[Conclusions](#)[References](#)[Tables](#)[Figures](#)[◀](#)[▶](#)[◀](#)[▶](#)[Back](#)[Close](#)[Full Screen / Esc](#)[Printer-friendly Version](#)[Interactive Discussion](#)

Terrestrial responses of low-latitude Asia to the Eocene–Oligocene climate transition

Y.-X. Li et al.

[Title Page](#)

[Abstract](#)

[Introduction](#)

[Conclusions](#)

[References](#)

[Tables](#)

[Figures](#)

[⏪](#)

[⏩](#)

[◀](#)

[▶](#)

[Back](#)

[Close](#)

[Full Screen / Esc](#)

[Printer-friendly Version](#)

[Interactive Discussion](#)

or 380 °C that decays toward the origin is regarded as a characteristic remanence (ChRM). The demagnetization data together with the rock magnetic data (Sect. 4.2.2) suggest that the remanence in the Youganwo oil shale is mainly carried by iron sulfides, probably greigite, while titanomagnetite is probably also the remanence carrier of the brown grey shale in the uppermost part of the Youganwo Fm and the mudstones of the overlying Huangniuling Fm.

To obtain reliable estimates of the ChRMs, the following criteria are also used to scrutinize the data: (a) we generally accept ChRMs of higher coercivity/unblocking temperature component decaying toward the origin with at least four data points; (b) ChRMs with a maximum angular deviation (MAD) greater than 16° are rejected; (c) if two samples from the same stratigraphic level yield similar ChRMs, the sample that has a better definition of the ChRM is used. Following the above treatments, we obtain reliable paleomagnetic data from 63 stratigraphic levels. Among these data, ChRMs from 46 stratigraphic levels have their corresponding virtual geomagnetic pole (VGP) within 45° from the mean of VGPs. These 46 ChRMs show both normal and reversed polarities (Fig. 6). A reversal test was performed and passed at 95 % confidence level with class “C” (McFadden and McElhinny, 1990). Therefore, the quality of the 46 ChRMs is ranked at “A” and the remaining 17 ChRMs are ranked at “B” in quality. Changes in inclinations and VGP latitudes of these ChRMs with depth are shown in Fig. 7c and d.

5 Discussions

5.1 Definition of magnetozones

Oil shales in the Youganwo Fm exhibit predominantly oblate AMS fabrics (Fig. 3), indicative of a depositional origin of the fabrics. Silty mudstone layers in the Huangniuling Fm also show mainly oblate AMS fabrics, and prolate fabrics occur as well, though weak. These features indicate depositional type of fabrics developed in the presence of currents flowing at a moderate speed (Tauxe, 1998), which is consistent with a deltaic

Terrestrial responses of low-latitude Asia to the Eocene–Oligocene climate transition

Y.-X. Li et al.

Title Page

Abstract

Introduction

Conclusions

References

Tables

Figures

◀

▶

◀

▶

Back

Close

Full Screen / Esc

Printer-friendly Version

Interactive Discussion

depositional environment for the Huangniuling Fm. In addition, reversed polarities are present and a reversal test passed (Sect. 4.3). Taking together, the occurrence of depositional type fabrics, the presence of reversed polarities, and the passage of a reversal test suggest that the remanence is likely primary. Therefore, both the VGP latitudes and inclinations are used to define magnetozones of the investigated section (Fig. 7e). Also, definition of magnetozones is primarily based on the “A”-quality ChRM data and the “B”-quality ChRM data are only used as a second-order constraint for intervals where “A”-quality data are sparse (Fig. 7c and d). In addition, a polarity zone is defined by at least two consecutive levels of same polarities. Changes in inclinations and VGP latitudes with depth are largely in concert, which allows us to define two reversed polarity zones (R1 and R2) and two main normal polarity zones (N1 and N2) (Fig. 7e). Among these magnetozones N1 and R2 are better defined. N1 is defined between 32.2 and 51.0 m, and R2 is defined from 25.0 to 32.2 m (Fig. 7e). Below 25.0 m is dominated by the normal polarities except at ~ 10 m where isolated negative inclinations and VGP latitudes occur (Fig. 7c and d). Although these negative values do not occur consecutively in depth (Fig. 7c and d), the trend of shift toward negative values in both inclinations and VGP latitudes is evident and is consistent, suggesting that a reversed polarity probably exists at ~ 10 m (Fig. 7e). This possible reversed polarity zone is tentatively defined between ~ 11.0 and ~ 8.5 m and separates the lower 25 m section into two short normal polarity zones, N2 and N3 (Fig. 7e).

5.2 Major constraints on a geomagnetic polarity timescale (GPTS)

Correlation of these magnetozones to the standard GPTS is not unique due to the lack of numerical ages serving as anchor points. However, several constraints exist for the investigated section. When these constraints are used collectively and in conjunction with the defined magnetozones (Fig. 7e), it is possible to establish a reliable polarity time scale for this section.

The major constraints are as follows. First, the studied oil shales contain abundant vertebrate and plant fossils (Chow and Liu, 1955; Liu, 1957; Yeh, 1958; Chow and Yeh,

Terrestrial responses of low-latitude Asia to the Eocene–Oligocene climate transition

Y.-X. Li et al.

[Title Page](#)

[Abstract](#)

[Introduction](#)

[Conclusions](#)

[References](#)

[Tables](#)

[Figures](#)

[◀](#)

[▶](#)

[◀](#)

[▶](#)

[Back](#)

[Close](#)

[Full Screen / Esc](#)

[Printer-friendly Version](#)

[Interactive Discussion](#)

1962; Li, 1975; Yu and Zu, 1983; Wang et al., 2007; Claude et al., 2012; Feng et al., 2012, 2013). In particular, the mammal fossil (*Lunania* cf. *L. youngi*) (Wang et al., 2007), which was unearthed from the studied oil shale of the Youganwo Fm, provides the most definitive evidence for a late Eocene age (Wang et al., 2007; Jin et al., 2008). Accordingly, the Youganwo oil shale was formed sometime in the Priabonian stage and/or Bartonian stage of the Eocene that could span from magnetic chrons C18r to C13r, i.e., 41 to 34 Ma (Fig. 7f). Second, the marked difference in lithology of the Youganwo Fm and the Huangniuling Fm suggests drastic difference in sediment accumulation rates. The sampled Youganwo Fm consists predominantly of brown oil shales; whereas the overlying Huangniuling Fm comprises dominantly massive pebbly coarse sandstones and siltstones. Therefore, the sediment accumulation rates for the Huangniuling Fm were much faster than those for the Youganwo Fm. In addition, although organic matter and silt content decreases upsection and grey mudstones occur at the uppermost of the Youganwo Fm, changes in sediment composition within the Youganwo Fm are subtle. This suggests that sediment accumulation rates of the studied Youganwo Fm should not change drastically. Third, the deposition between the Youganwo and Huangniuling Fms is continuous. The contact between the two formations displays a continuous, gradual change from brown grey mudstones at the uppermost Youganwo Fm to pale grey mudstones at the base of the Huangniuling Fm within an interval of ~ 50 cm. In addition, siltstones and sandstones overlying the basal pale grey mudstone exhibit a coarsening upward trend in grain size, indicating a continuous deposition during the transition from the Youganwo Fm to the Huangniuling Fm. Fourth, the characteristic sedimentary rhythms of the investigated section may also be used as an additional constraint. The occurrence of sedimentary rhythms is not unique at the studied section. A marine succession of similar age in Massignano, Italy also displays striking limestone/marl cycles (Jovane et al., 2006). Cyclic lithologic patterns are also seen in the Middle Eocene oil shale-bearing lacustrine succession in the Mudurnu-Göynük Basin, Turkey (Ocakoglu et al., 2012), the Eocene oil shale-bearing Green River Formation in the United States (Meyers, 2008), and other terrestrial records of similar ages

in Asia (e.g., Dupont-Nivet et al., 2007; Xiao et al., 2010). All these lithologic cycles are attributed to orbital forcing and represent orbital cycles (Jovane et al., 2006; Dupont-Nivet et al., 2007; Meyers, 2008; Xiao et al., 2010; Ocakoglu et al., 2012). The strong lithologic expression of orbital variations in both marine and terrestrial records, particularly those containing oil shales, from widespread regions at similar ages leads us to believe that the sedimentary cycles of the studied section likely represent orbital cycles as well. Although it is not certain yet as to which orbital cycle(s) (i.e., eccentricity, obliquity, or precession) these sedimentary rhythms may represent, the frequency of these lithologic cycles should be within the orbital frequency band, which can be used as an additional, first-order constraint when establishing a time scale for the studied section. Based on the definition of the magnetozones (Fig. 7), there are ~ 3.5 sedimentary cycles in N1. Because a sedimentary cycle in the Huangniuling Fm is represented by a sequence of red layer, massive sandstone, and a thin mudstone, one red layer marker at 40 m might be unidentified, where the accompanied thin mudstone bed did occur (Fig. 7). Therefore, there are probably 4 sedimentary cycles in N1 zone. Similarly, there are ~ 3 sedimentary cycles in R2 zone and ~ 8.5 sedimentary cycles in N2 zone, respectively (Fig. 7).

5.3 Construction of a geomagnetic polarity timescale (GPTS)

With aforementioned constraints, correlations between the four polarity zones (Fig. 7e) and the magnetochrons C18r to C13r (Fig. 7f) can be examined and unrealistic correlations can be rejected. Because polarity zones N1 and R2 are better defined than other two polarity zones, correlation is thus constructed mainly between the N1 + R2 pair and the consecutive normal + reversed magnetochrons of the GPTS. To facilitate the analyses, the N2 zone is also used, but as a secondary constraint, in establishing the correlations.

The results of correlations are summarized in Table 1. With the first-order constraint that the Youganwo oil shales were formed in the Late Eocene, six ensembles of correlations are possible between the N1 + R2 pair and the normal-reversed magnetochron

CPD

11, 2811–2845, 2015

Terrestrial responses of low-latitude Asia to the Eocene–Oligocene climate transition

Y.-X. Li et al.

Title Page

Abstract

Introduction

Conclusions

References

Tables

Figures

◀

▶

◀

▶

Back

Close

Full Screen / Esc

Printer-friendly Version

Interactive Discussion



Terrestrial responses of low-latitude Asia to the Eocene–Oligocene climate transition

Y.-X. Li et al.

Title Page

Abstract

Introduction

Conclusions

References

Tables

Figures

◀

▶

◀

▶

Back

Close

Full Screen / Esc

Printer-friendly Version

Interactive Discussion

pairs in the Late Eocene, i.e., from C18 to C13 (Table 1). The quality of each correlation is examined as follows. Ensemble 1 correlates N1 and R2 zones with C18n and C18r, respectively. This correlation would force the majority of the Youganwo oil shale section (N2–N3), where funa fossils of Late Eocene age were discovered, to the Middle Eocene (Fig. 7e and f). Therefore, ensemble 1 is rejected. Ensemble 2 correlates N1 and R2 zones with C17n and C17r, respectively. The corresponding sedimentation rates for N1 and R2 are 1.38 and 2.54 cm kyr^{-1} , respectively (Table 1). Ensemble 2 is rejected on the grounds that (1) the 1.38 cm kyr^{-1} for N1 is too slow for the massive pebbly coarse sandstones; and (2) the 1.38 cm kyr^{-1} for N1 is slower than the 2.54 cm kyr^{-1} for R2 in the oil shales. Ensemble 3 relates N1 to C16n.2n and R2 to C16r. Such a correlation would yield a sedimentation rate of 2.90 cm kyr^{-1} for N1 and 2.68 cm kyr^{-1} for R2 (Table 1). Because the 2.90 cm kyr^{-1} rate of N1 in coarse sandstones of the Huangniuling Fm is similar to the 2.68 cm kyr^{-1} rate of R2 in the oil shale, which is unrealistic, ensemble 3 is rejected as well. Ensemble 4 links N1 to C16n.1n, R2 to C16n.1r, and N2 to C16n.2n. This correlation leads to a sedimentation rate of 10.11 cm kyr^{-1} for N1, 4.53 cm kyr^{-1} for R2 in the upper part of the Youganwo Fm, 2.31 cm kyr^{-1} for N2.1n in the lower part of the Youganwo Fm (Table 1). Although the fact that the 10.11 cm kyr^{-1} rate for N1 is much faster than the 4.53 cm kyr^{-1} for R2 is well compatible with the lithology, the sedimentation rate for the upper part of the Youganwo Fm (R2) is almost two times of that for the lower part of the Youganwo oil shale. The sedimentation rate difference is too large to be compatible with the subtle compositional change in the studied Youganwo Fm. For this reason, ensemble 4 is also rejected.

In ensemble 5, N1 and R2 zones are correlated to C15n and C15r, respectively. Assuming that C16n.1r was not captured probably due to its relatively short duration, N2 zone would correlate to C16n. Such a correlation yields a sedimentation rate of ~ 6.37 cm kyr^{-1} for N1, ~ 1.75 cm kyr^{-1} for R2, and ~ 1.51 cm kyr^{-1} for N2 (Table 1). These sedimentation rates comply with the constraints in Sect. 5.2, i.e., (1) the sedimentation rate for N1 in the coarse sandstones in the Huangniuling Fm should be much faster than that for R2 in the upper part of the Youganwo Fm; (2) sedimentation rates

Terrestrial responses of low-latitude Asia to the Eocene–Oligocene climate transition

Y.-X. Li et al.

Title Page

Abstract

Introduction

Conclusions

References

Tables

Figures

◀

▶

◀

▶

Back

Close

Full Screen / Esc

Printer-friendly Version

Interactive Discussion

val. There are two ways to estimate the duration of the 1.2 m thick interval. One is to extrapolate the sedimentation rate of $\sim 0.56 \text{ cm kyr}^{-1}$ for the uppermost part of the Youganwo Fm, i.e., R2 zone. This would lead to an estimate of $\sim 210 \text{ kyr}$ and the onset of the transition is then estimated to be at $\sim 33.915 \text{ Ma}$. The second approach is to treat the 1.2 m thick interval as the upper part of the long eccentricity cycle at the uppermost of the Youganwo Fm (Fig. 7a and b). This results in an estimate of $\sim 140 \text{ kyr}$ for the 1.2 m thick interval and an onset age of $\sim 33.845 \text{ Ma}$. Taking the average of the above two estimates, we obtain a mean age of 33.88 Ma for the onset of the transition.

The constructed timescale represents a significantly refined chronology for the Paleogene strata in the Maoming Basin. It not only provides the tightest possible constraints on the timing of the onset of the transition from a lacustrine environment to a deltaic environment in the Maoming Basin, but also permits detailed dating of the studied section. Because there are 19 parasequences, which probably represent 19 short eccentricity cycles, in the exposed Huangniuling Fm, the duration of the exposed Huangniuling Fm is estimated to be $\sim 1.9 \text{ Myr}$ and the age of the uppermost of the section (Fig. 2a) is estimated at $\sim 31.98 \text{ Ma}$. The age of the uppermost of the magnetostratigraphic section (Fig. 7) would be $\sim 33.2 \text{ Ma}$. For the Youganwo Fm, the R2 magnetozone is correlated to magnetochron C13r and the basal age of R2 magnetozone is at 34.999 Ma . Since the N2 zone is correlated to magnetochrons C15n–C17n, the basal age of N2 zone would be at 38.333 Ma . Since there are 3 or 4 sedimentary cycles (Fig. 2), which probably represent long eccentricity cycles, in the lower $\sim 11 \text{ m}$ section below the N2 magnetozone, the basal age of the investigated section is estimated to be at $\sim 39.73 \text{ Ma}$.

5.4 Paleoclimatic implications

The rapid transition from a lacustrine environment to a deltaic environment and the subsequent persistently prolonged drying conditions could be related to global climate change. In the late Paleogene, the Earth's climate underwent a major transition from greenhouse to icehouse that was climaxed at the Eocene–Oligocene boundary (Za-

Terrestrial responses of low-latitude Asia to the Eocene–Oligocene climate transition

Y.-X. Li et al.

Title Page

Abstract

Introduction

Conclusions

References

Tables

Figures



Back

Close

Full Screen / Esc

Printer-friendly Version

Interactive Discussion

is dominated by coarse sandstones and exhibits sedimentary rhythms that are characterized by the repeated occurrence of a parasequence containing red sandstone layer, massive coarse sandstones, and a relatively thin mudstone layer. The sedimentary cycles in the Huangniuling Fm are linked to short eccentricity cycles (~ 100 kyr) in the chronologic framework. The exposed Huangniuling Fm contains 19 such sedimentary cycles and is bracketed between ~ 33.88 and ~ 31.98 Ma.

The contact between the Youganwo Fm and the Huangniuling Fm is represented by a 50 cm interval that shows a gradual change from dark grey mudstone at the uppermost of the Youganwo Fm to the grey mudstone and siltstones with a coarsening upward trend in grain size at the base of the Huangniuling Fm. This interval represents a major environment change from a lacustrine to a deltaic environment in the Maoming Basin and its onset is dated at ~ 33.88 Ma. The timing of the onset of the dramatic environmental change is in remarkable similarity with that of the Eocene–Oligocene transition (EOT) that is dated at 33.7 to 33.9 Ma from various marine records. The synchronicity suggests strong linkage between these two events and implies that the rapid environmental change in the Maoming Basin most likely represents terrestrial responses to the global cooling associated with the EOT. This notion is strengthened by the subsequent occurrence of the persistently prolonged dry conditions, as represented by the ~ 1.9 Myr Huangniuling coarse sandstones, following the rapid environment change coincident with the EOT. These features are highly compatible with the continued deteriorating conditions after the EOT.

Acknowledgements. This study was supported by National Natural Science Foundation of China (Nos. 41210001, 41372002, 41274071, 41230208, 41321062), the National Basic Research Program of China (No. 2012CB822000), and the Fundamental Research Funds for the Central Universities (20620140389). We thank Shipeng Wang for field assistance, Mike Jackson and Qingsong Liu for helpful discussions about the rock magnetic data.

References

- Aleksandrova, G. N., Kodrul, T. M., Liu, X. Y., Song, Y. S., and Jin, J. H.: Palynological characteristics of the upper part of the Youganwo Formation and lower part of the Huangniuling Formation, Maoming Basin, South China, in: Proceedings of the 2nd Sino-Russian Seminar on Evolution and Development of Eastern Asia Flora based on Palaeobotanical Data, Guangzhou, China. School of Life Sciences, Sun Yat-sen University, Guangzhou, China, 3–15, 2012.
- Bohaty, S. M., Zachos, J. C., and Delaney, L. M.: Foraminiferal Mg/Ca evidence for Southern Ocean cooling across the Eocene–Oligocene transition, *Earth Planet. Sc. Lett.*, 317–318, 251–261, 2012.
- Bureau of Geology and Mineral Resources of Guangdong Province: Regional Geology of Guangdong Province, Geological Publishing House, Beijing, (in Chinese with English abstract) 1988.
- Bureau of Geology and Mineral Resources of Guangdong Province: Stratigraphy (Lithostratic) of Guangdong Province, China University of Geosciences Press, Wuhan, (in Chinese) 1996.
- Brown, R. E., Koeberl, C., Montanari, A., and Bice, D. M.: Evidence for a change in Milankovitch forcing caused by extraterrestrial events at Massignano, Italy, Eocene–Oligocene boundary GSSP, in: *The Late Eocene Earth – Hothouse, Icehouse and Impacts*, edited by: Koeberl, C., and Montanari, A., *Geol. S. Am. S.*, 452, 119–137, doi:10.1130/2009.2452(08), 2009.
- Chow, M. C. and Liu, C. L.: A new anostherine turtle from Maoming, Kwangtung, *Acta Palaeontol. Sinica*, 3, 275–282, (in Chinese with English abstract) 1955.
- Chow, M. C. and Yeh, H. K.: A new emydid from the Eocene of Maoming, Kwangtung, *Vertebrat. Palasiatic.*, 6, 225–229, (in Chinese with English abstract) 1962.
- Claude, J., Zhang, J. Y., Li, J. J., Mo, J. Y., Kuang, X. W., and Tong, H. Y.: Geoemydid turtles from the Late Eocene Maoming basin, southern China, *B. Soc. Geol. Fr.*, 183, 641–651, 2012.
- Coxall, H. K., Wilson, P. A., Pälike, H., Lear, C. H., and Backman, J.: Rapid stepwise onset of Antarctic glaciation and deeper calcite compensation in the Pacific Ocean, *Nature*, 433, 53–57, 2005.
- Cotton, L. J. and Pearson, P. N.: Extinction of larger benthic foraminifera at the Eocene/Oligocene boundary, *Palaeogeogr. Palaeoclimatol.*, 311, 281–296, 2011.

Terrestrial responses of low-latitude Asia to the Eocene–Oligocene climate transition

Y.-X. Li et al.

Title Page

Abstract

Introduction

Conclusions

References

Tables

Figures

◀

▶

◀

▶

Back

Close

Full Screen / Esc

Printer-friendly Version

Interactive Discussion



**Terrestrial responses
of low-latitude Asia to
the
Eocene–Oligocene
climate transition**Y.-X. Li et al.

[Title Page](#)[Abstract](#)[Introduction](#)[Conclusions](#)[References](#)[Tables](#)[Figures](#)[Back](#)[Close](#)[Full Screen / Esc](#)[Printer-friendly Version](#)[Interactive Discussion](#)

Jovane, L., Florindo, F., Sprovieri, M., and Pälike, H.: Astronomic calibration of the late Eocene/early Oligocene Massignano section (central Italy), *Geochem. Geophys. Geos.*, 7, Q07012, doi:10.1029/2005GC001195, 2006.

Kirschvink, J. L.: The least-squares line and plane and the analysis of paleomagnetic data, *Geophys. J. Int.*, 62, 699–718, doi:10.1111/j.1365-246X.1980.tb02601.x, 1980.

Li, J. L.: New materials of *Tomistoma petrolica* Yeh from Maoming, Guangdong, *Vertebrat. Palasiatic.*, 13, 190–194, (in Chinese) 1975.

Li, Y. X., Bralower, T. J., Montanez, I. P., Osleger, D. A., Arthur, M. A., Bice, D. M., Herbert, T. D., Erba, E., and Premoli-Silva, I.: Toward an orbital chronology for the early Aptian Oceanic Anoxic Event 1a (OAE1a, ~120Ma), *Earth Planet. Sc. Lett.*, 271, 88–100, doi:10.1016/j.epsl.2008.03.055, 2008.

Licht, A., van Cappelle, M., Abels, H. A., Ladant, J.-B., Trabucho-Alexandre, J., and France-Lanord, C.: Asian monsoons in a late Eocene greenhouse world, *Nature*, 513, 501–506, doi:10.1038/nature13704, 2014.

Licht, A., Boura, A., De Franceschi, D., Utescher, T., Sein, C., and Jaeger, J.-J.: Late middle Eocene fossil wood of Myanmar: implications for the landscape and the climate of the Eocene Bengal Bay. *Rev. Palaeobot. Palyno.*, 216, 44–54, 2015.

Liu, X. T.: A new fossil cyprinid fish from Maoming, Kwangtung, *Vertebrat. Palasiatic.*, 1, 151–153, (in Chinese with English abstract) 1957.

Liu, Z. H., Pagani, M., Zinniker, D., DeConto, R., Huber, M., Brinkhuis, H., Shah, S. R., Leckie, R. M., and Pearson, A.: Global cooling during the Eocene–Oligocene climate transition, *Science*, 323, 1187–1190, 2009.

Lurcock, P. C. and Wilson, G. S.: PuffinPlot: a versatile, user-friendly program for paleomagnetic analysis, *Geochem. Geophys. Geos.*, 13, Q06Z45, doi:10.1029/2012GC004098, 2012.

McFadden, P. L. and McElhinny, M. W.: Classification of the reversal test in palaeomagnetism, *Geophys. J. Int.*, 103, 725–729, 1990.

Meyers, S. R.: Resolving Milankovitchian controversies: the Triassic latemar limestone and the Eocene green river formation, *Geology*, 36, 319–322, doi:10.1130/G24423A.1, 2008.

Ocakoglu, F., Açikalin, S., Yılmaz, I. Ö., Safak, Ü., and Gökçeoglu, C.: Evidence of orbital forcing in lake-level fluctuations in the Middle Eocene oil shale-bearing lacustrine successions in the Mudurnu–Göynük Basin, NW Anatolia (Turkey), *J. Asian Earth Sci.*, 56, 54–71, 2012.

Terrestrial responses of low-latitude Asia to the Eocene–Oligocene climate transition

Y.-X. Li et al.

[Title Page](#)
[Abstract](#)
[Introduction](#)
[Conclusions](#)
[References](#)
[Tables](#)
[Figures](#)




[Back](#)
[Close](#)
[Full Screen / Esc](#)
[Printer-friendly Version](#)
[Interactive Discussion](#)

Ogg, J. G.: Geomagnetic polarity time scale, in: *The Geologic Time Scale 2012*, Chapter 5, edited by: Gradstein, F. M., Ogg, J. G., Schmitz, M. D., and Ogg, G. M., Elsevier, Amsterdam, 85–113, 2012.

Oskolski, A. A., Feng, X. X., and Jin, J. H.: Myrtineoxylon gen. nov.: the first fossil wood record of the tribe Myrteae (Myrtaceae) in eastern Asia, *Taxon*, 62, 771–778, 2013.

Pälike, H., Norris, R. D., Herrle, J. O., Wilson, P. A., Coxall, H. K., Lear, C. H., Shackleton, N. J., Tripathi, A. K., and Wade, B. S.: The heartbeat of the Oligocene climate system, *Science*, 314, 1894–1898, doi:10.1126/science.1133822, 2006.

Pälike, H., Lyle, M. W., Nishi, H., Raffi, I., Ridgwell, A., and Gamage, K., Klaus, A., Acton, G., Anderson, L., Backman, J., Baldauf, J., Beltran, C., Bohaty, S. M., Bown, P., Busch, W., Channell, J. E. T., Chun, C. O. J., Delaney, M., Dewangan, P., Dunkley Jones, T., Edgar, K. M., Evans, H., Fitch, P., Foster, G. L., Gussone, N., Hasegawa, H., Hathorne, E. C., Hayashi, H., Herrle, J. O., Holbourn, A., Hovan, S., Hyeong, K., Iijima, K., Ito, T., Kamikuri, S.-i., Kimoto, K., Kuroda, J., Leon-Rodriguez, L., Malinverno, A., Moore Jr., T. C., Murphy, B. H., Murphy, D. P., Nakamura, H., Ogane, K., Ohneiser, C., Richter, C., Robinson, R., Rohling, E. J., Romero, O., Sawada, K., Scher, H., Schneider, L., Sluijs, A., Takata, H., Tian, J., Tsujimoto, A., Wade, B. S., Westerhold, T., Wilkens, R., Williams, T., Wilson, P. A., Yamamoto, Y., Yamamoto, S., Yamazaki, T., and Zeebe, R. E.: A Cenozoic record of the equatorial Pacific carbonate compensation depth, *Nature*, 488, 609–614, doi:10.1038/nature11360, 2012.

Pearson, P. N., McMillan, I. K., Wade, B. S., Dunkley Jones, T., Coxall, H. K., Bown, P. R., and Lear, C. H.: Extinction and environmental change across the Eocene–Oligocene boundary in Tanzania, *Geology*, 36, 179–182, 2008.

Prothero, D. R.: The late Eocene–Oligocene extinctions, *Annu. Rev. Earth Pl. Sc.*, 22, 145–165, 1994.

Quan, C., Liu, Z. H., Utescher, T., Jin, J. H., Shu, J. W., Li, Y. X., and Liu, Y.-S. C.: Revisiting the Paleogene climate pattern of East Asia: a synthetic review, *Earth-Sci. Rev.*, 139, 213–230, 2014.

Quan, C., Liu, Y.-S. C., and Utescher, T.: Eocene monsoon prevalence over China: a paleobotanical perspective, *Palaeogeogr. Palaeoclimatol.*, 365–366, 302–311, 2012.

Roberts, A. P., Chang, L., Rowan, C. J., Horng, C.-S., and Florindo, F.: Magnetic properties of sedimentary greigite (Fe₃S₄): an update, *Rev. Geophys.*, 49, RG1002, doi:10.1029/2010RG000336, 2011.

**Terrestrial responses
of low-latitude Asia to
the
Eocene–Oligocene
climate transition**

Y.-X. Li et al.

[Title Page](#)[Abstract](#)[Introduction](#)[Conclusions](#)[References](#)[Tables](#)[Figures](#)[Back](#)[Close](#)[Full Screen / Esc](#)[Printer-friendly Version](#)[Interactive Discussion](#)

- Yu, J. F. and Wu, Z. J.: Spore-pollen assemblage of Mao 5 well of Maoming Basin, Guangdong and its geological age, *Journal of Stratigraphy*, 7, 112–118, (in Chinese) 1983.
- Zachos, J. C., Pagani, M., Sloan, L., Thomas, E., and Billups, K.: Trends, rhythms, and aberrations in global climate 65 Ma to present, *Science*, 292, 686–693, 2001.
- 5 Zanazzi, A., Kohn, M. J., MacFadden, B. J., and Terry, D. O. Jr.: Large temperature drop across the Eocene–Oligocene transition in central North America, *Nature*, 445, 639–642, 2007.
- Zijderveld, J. D. A.: A. C. demagnetization of rocks: analysis of results, in: *Methods in Palaeomagnetism*, edited by: Collinson, D. W., Creer, K. M., and Runcorn, S. K.: Elsevier, Amsterdam, 254–286, 1967.

Terrestrial responses of low-latitude Asia to the Eocene–Oligocene climate transition

Y.-X. Li et al.

Table 1. Correlations of magnetozones with chrons of C18 to C13 of the geomagnetic polarity time scale (GPTS).

Correlations	1		2		3		4		5		6				
Polarity zone(chron (Depth, <i>n</i> cycles)\(myr)	C18n	C18r	C17n	C17r	C16n.2n	C16r	C16n.1n	C16n.1r	C16n.2n	C15n	C15r	C16n	C13n	C13r	C15n-C17n
N1 (32.2–51.0 m, ~ 4)	1.23	–	1.38	–	2.90	–	10.11	–	–	6.37	–	–	3.43	–	–
R2 (25.0–32.2 m, ~ 3)	–	0.71	–	2.54	–	2.68	–	4.53	–	–	1.75	–	–	0.56	–
N2 (25.0–11.0 m, ~ 8.5)	–	–	–	–	–	–	–	–	2.31	–	–	1.51	–	–	0.42
Periodicity of cycle (kyr)	382	337	341	94	162	90	47	53	76	74	137	117	137	431	392
Remark	x ^a		x ^b		x ^b		x ^c		x ^d		x ^d		x ^e		

Note: Boldface/normal font stands for the reversed/normal polarity zones/chrons; depths are in m.

n = number of sedimentary cycles.

Sedimentation rates in the table are in cm kyr⁻¹.

"–" denotes "not applicable"; "x" indicates that the correlation is unrealistic and is rejected. "✓" indicates acceptable correlations.

a–e provides brief comments on why the correlation is rejected or accepted.

^a the correlation would place the majority of the Youganwo Fm, i.e., N2-N3, to the Middle Eocene.

^b the correlation would result in sedimentation rates in R2, i.e., the Youganwo Fm, faster than or similar to those in N1, i.e., the Huangniuling Fm.

^c the correlation leads to the drastic difference in sedimentation rates between the upper (R2) and lower (N2) part of the studied Youganwo Fm.

^d the sedimentation rates for the Youganwo oil shale are too fast in comparison to those of well-dated organic-rich shales in deep-time.

^e the sedimentation rates of the Youganwo oil shale are compatible with those of well-dated organic-rich shales in deep-time and the sedimentary cycles in both Huangniuling Fm (N1) and the Youganwan Fm (R2 and N2) are in the orbital frequency bands and likely represent eccentricity cycles, see text for details.

Title Page

Abstract

Introduction

Conclusions

References

Tables

Figures

◀

▶

◀

▶

Back

Close

Full Screen / Esc

Printer-friendly Version

Interactive Discussion



Terrestrial responses of low-latitude Asia to the Eocene–Oligocene climate transition

Y.-X. Li et al.

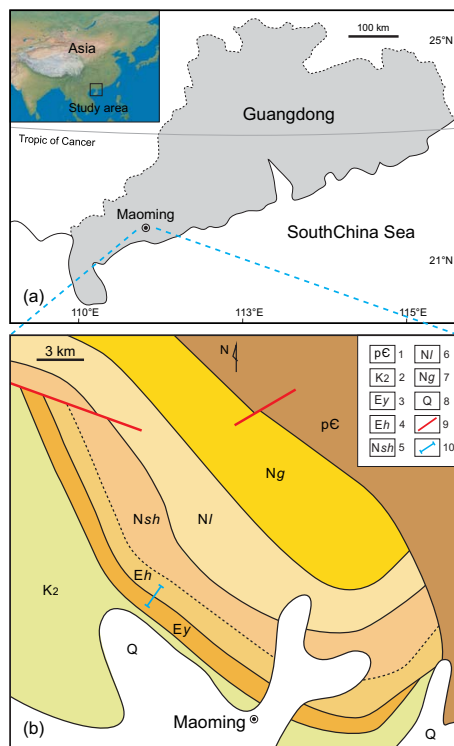


Figure 1. Location and regional geology of the study area. **(a)** Map showing the location of the Maoming Basin, Guangdong Province, southern China. **(b)** Simplified geological map of the Maoming Basin. 1. Precambrian; 2. Upper Cretaceous; 3. Youganwo Fm.; 4. Huangniuling Fm.; 5. Shangcun Fm.; 6. Laohuling Fm.; 7. Gaopengling Fm.; 8. Quaternary; 9. Fault; 10. Investigated Jintang section.

[Title Page](#)
[Abstract](#)
[Introduction](#)
[Conclusions](#)
[References](#)
[Tables](#)
[Figures](#)
[◀](#)
[▶](#)
[◀](#)
[▶](#)
[Back](#)
[Close](#)
[Full Screen / Esc](#)
[Printer-friendly Version](#)
[Interactive Discussion](#)

Terrestrial responses of low-latitude Asia to the Eocene–Oligocene climate transition

Y.-X. Li et al.

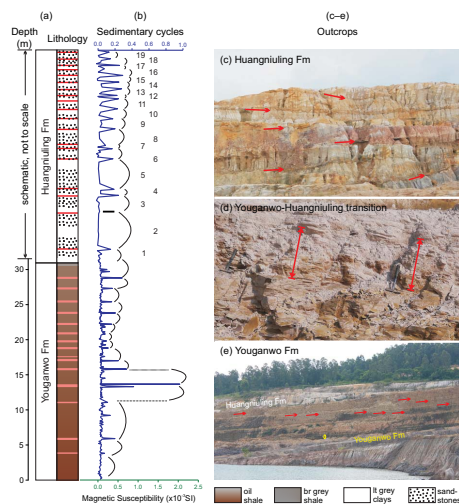


Figure 2. Lithostratigraphic columns **(a)**, sedimentary cycles **(b)**, and field photographs **(c–e)** of the investigated section exposed in the now-abandoned open mine pit in Maoming Basin. The Huangniuling Fm part of the stratigraphic column schematically shows the overall rhythmic sedimentary feature that is characterized by the occurrence of a thin bed (shown in short red lines) of red coarse sandstone at the base, followed by massive grey sandstone that is capped by light grey clays. The distinct thin red sandstone layer is numbered **(b)** and a total of 19 repeated sedimentary packages (cycles) are identified. The beds with distinct reddish color at distance in the Youganwo Fm are indicated by the pinkish lines and these beds generally correspond to the magnetic susceptibility peaks **(b)**. Note the different scales of the magnetic susceptibility of the Youganwo Fm (the lower part) and the Huangniuling Fm (the upper part) in **(b)**. In **(c)**, the red arrows indicate the red, thin marker bed of sandstone. In **(e)**, the yellow ellipse at the lower-middle part of the picture marks a person for scale; red arrows point to several distinctive reddish layers that form the sedimentary rhythms. br grey = brown grey, lt grey = light grey.

[Title Page](#)
[Abstract](#)
[Introduction](#)
[Conclusions](#)
[References](#)
[Tables](#)
[Figures](#)
[◀](#)
[▶](#)
[◀](#)
[▶](#)
[Back](#)
[Close](#)
[Full Screen / Esc](#)
[Printer-friendly Version](#)
[Interactive Discussion](#)

Terrestrial responses of low-latitude Asia to the Eocene–Oligocene climate transition

Y.-X. Li et al.

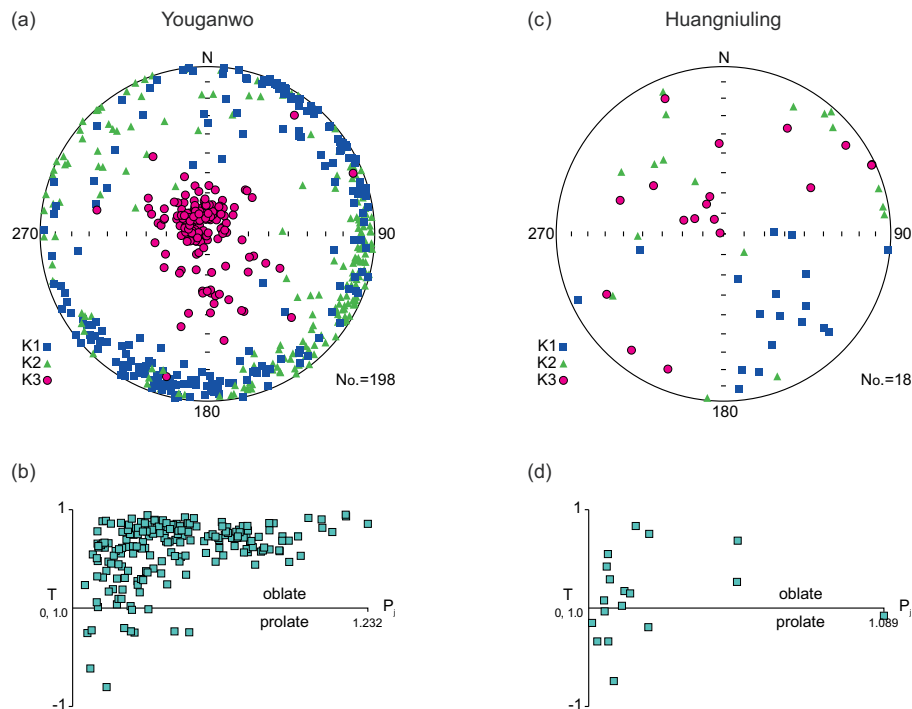


Figure 3. Anisotropy of magnetic susceptibility (AMS) data of the Youganwanwo Fm (a, b) and the Huangniuling Fm (c and d). k_1 , k_2 , k_3 are the maximum, intermediate, and minimum axis of the anisotropy ellipsoid, respectively. (a and c) are the equal area projection of these principal axes. No. is the number of specimens. T and P_j in (b and d) are the shape factor and the degree of anisotropy, respectively (Jelinek, 1981).

Terrestrial responses of low-latitude Asia to the Eocene–Oligocene climate transition

Y.-X. Li et al.

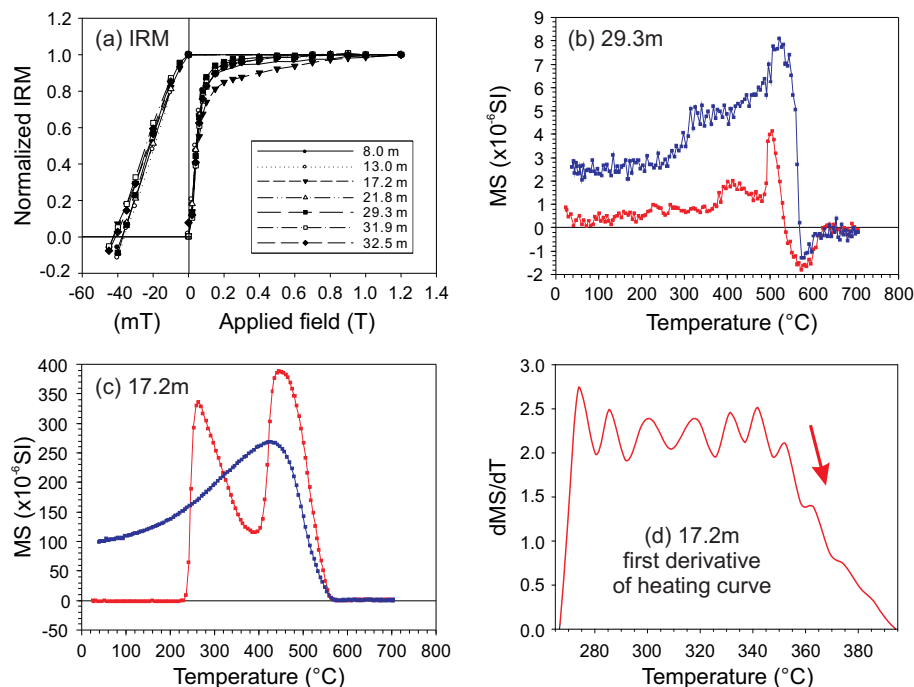


Figure 4. Rock magnetic data of samples from the Youganwo Fm and Huangniuling Fm. **(a)** IRM acquisition and the subsequent demagnetization in a backward field. **(b–d)** Thermal changes of magnetic susceptibility (MS) of samples from the uppermost brown grey shale (29.3 m) and the oil shale (17.2 m) of the Youganwo Fm. **(d)** shows the first derivative of the heating curve of **(c)** between 265 and 395 $^{\circ}$ C.

[Title Page](#)
[Abstract](#)
[Introduction](#)
[Conclusions](#)
[References](#)
[Tables](#)
[Figures](#)
[◀](#)
[▶](#)
[◀](#)
[▶](#)
[Back](#)
[Close](#)
[Full Screen / Esc](#)
[Printer-friendly Version](#)
[Interactive Discussion](#)

Terrestrial responses of low-latitude Asia to the Eocene–Oligocene climate transition

Y.-X. Li et al.

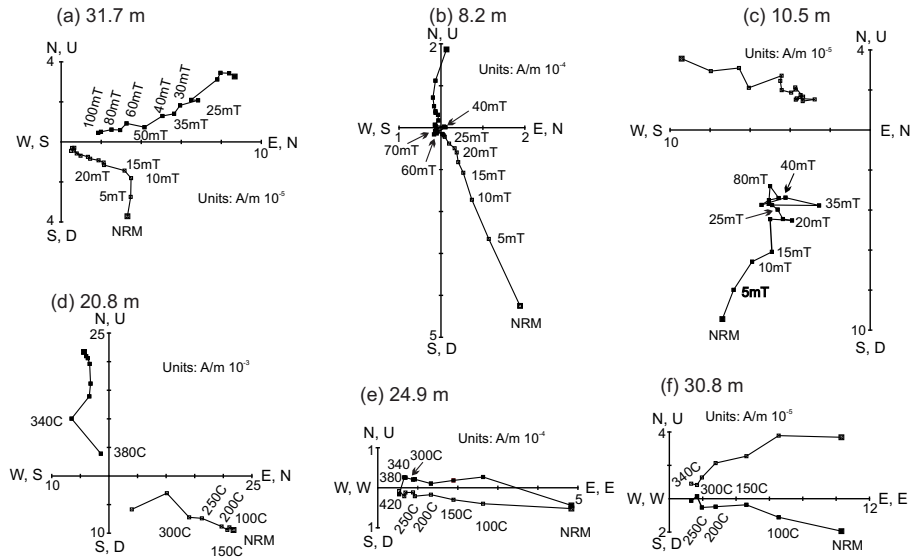


Figure 5. Representative demagnetization data of samples from the studied section. Open/closed squares indicate the vertical/horizontal components.

[Title Page](#)

[Abstract](#) | [Introduction](#)

[Conclusions](#) | [References](#)

[Tables](#) | [Figures](#)

[◀](#) | [▶](#)

[◀](#) | [▶](#)

[Back](#) | [Close](#)

[Full Screen / Esc](#)

[Printer-friendly Version](#)

[Interactive Discussion](#)



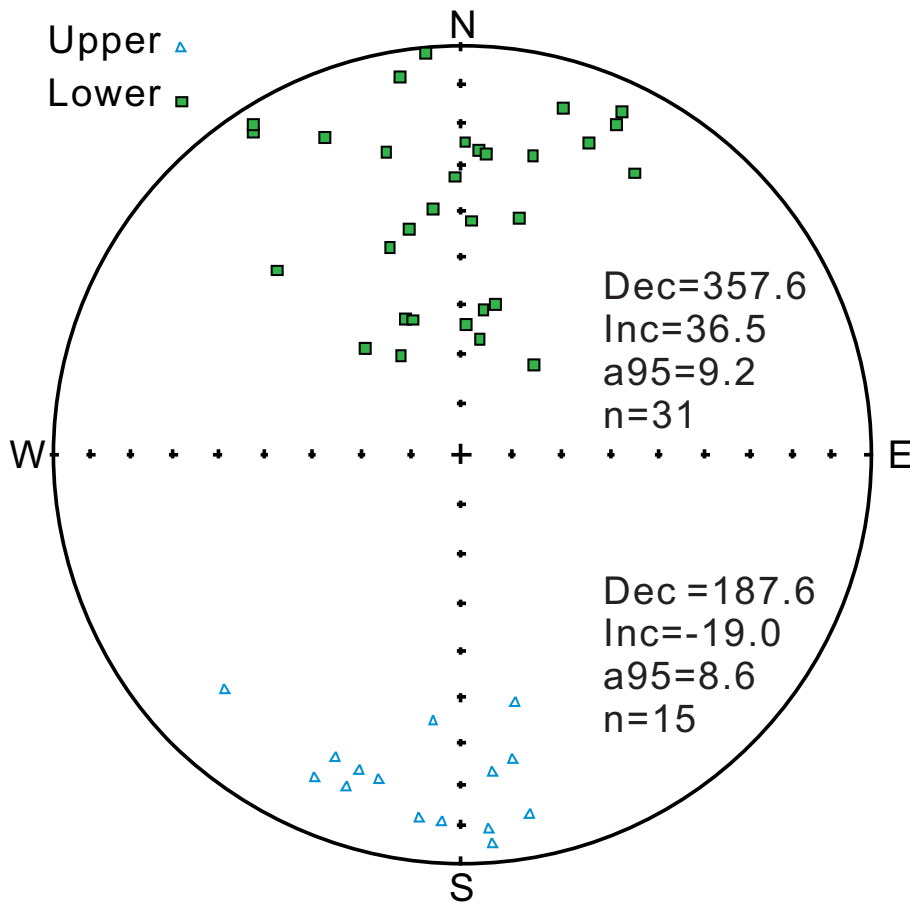


Figure 6. Characteristic remanent magnetization in stratigraphic coordinates. The solid/open symbols represent the lower/upper hemisphere projection.

**Terrestrial responses
of low-latitude Asia to
the
Eocene–Oligocene
climate transition**

Y.-X. Li et al.

[Title Page](#)

[Abstract](#)

[Introduction](#)

[Conclusions](#)

[References](#)

[Tables](#)

[Figures](#)

[◀](#)

[▶](#)

[◀](#)

[▶](#)

[Back](#)

[Close](#)

[Full Screen / Esc](#)

[Printer-friendly Version](#)

[Interactive Discussion](#)



Terrestrial responses of low-latitude Asia to the Eocene–Oligocene climatic transition

Y.-X. Li et al.

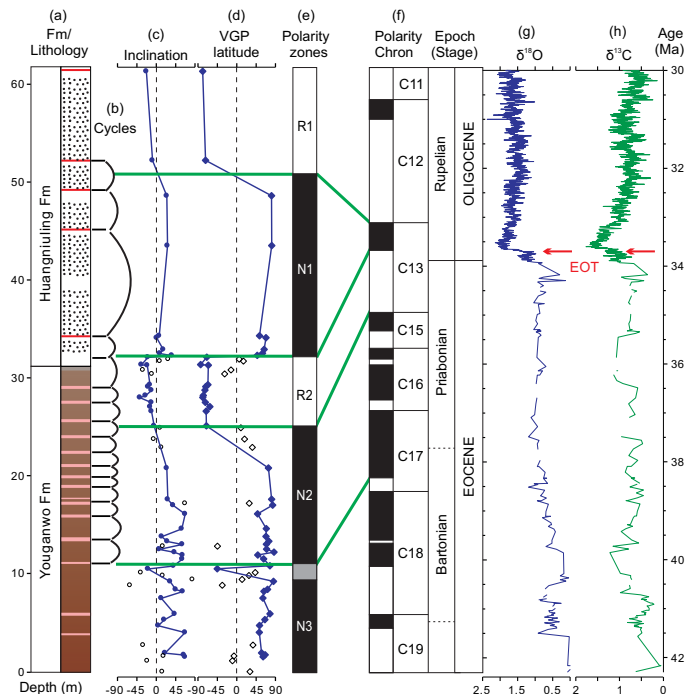


Figure 7. Integrated litho-, cyclo-, and magnetostratigraphy of the investigated section, and the correlation with the $\delta^{18}\text{O}$ and $\delta^{13}\text{C}$ records from the equatorial Pacific deep-sea sediments (ODP site 1218) (Pälike et al., 2006) that show the Eocene–Oligocene climatic transition (EOT). The legends for lithology and sedimentary cycles are the same as those in Fig. 2. In (c and d), the solid (open) symbols represent “A” (“B”)-quality ChRM data.

Title Page

Abstract

Introduction

Conclusions

References

Tables

Figures

◀

▶

◀

▶

Back

Close

Full Screen / Esc

Printer-friendly Version

Interactive Discussion